Available online at www.sciencedirect.com
SCIENCE DIRECT®
Journal of Power Sources 129 (2004) 216–228
JOURNAL OF POWER SOURCES
www.elsevier.com/locate/jpowsour

Ejector performance influence on a solid oxide fuel cell anodic recirculation system

F. Marsano, L. Magistri, A.F. Massardo*

Thermochemical Power Group (TPG)[1], Dipartimento di Macchine, Sistemi Energetici e Trasporti, Università di Genova, Via Montatallegro 1, Genova 16145, Italy

Received 18 June 2003; accepted 15 November 2003

Abstract

This work deals with the design and off-design performance evaluation of an anodic recirculation system based on ejector technology for solid oxide fuel cell hybrid applications.

The analysis presented here has been divided into three parts: (i) ejector design taking into account all the thermodynamic, fluid dynamic and chemical constraints, such as steam to carbon ratio (two ejector geometries have been considered: constant area mixing section, constant pressure mixing section); (ii) stand-alone ejector design and off-design performance analysis; (iii) influence on the whole hybrid system—SOFC, reformer, anode recirculation-design and off-design performance of the ejector primary flow conditions (hybrid system part-load conditions).

Keywords: Ejector; Anodic recirculation; SOFC

1. Introduction

Ejectors have been studied for many years, especially for applications in the alimentary industry, chemical industry, oil plants, and airplane jet propulsion [1–4]. In the ejector (Fig. 1) a primary fluid at high pressure expands in a nozzle and enters a duct, at high velocity, where it mixes with another gas (secondary or entrained fluid) coming in from a second line [1,5]. The two flows come into contact in the so-called mixing duct, where the driving fluid transfers part of its momentum to the secondary low-velocity flow. The mixing phase is considered complete when uniformity is reached from the point of view of the speed and temperature profiles (and in this case also the chemical composition profile). At this point the high-speed flow enters the diffuser to convert kinetic energy into pressure to reach a higher value than that of the secondary inlet one. In this sense the ejector operates as a compressor, but with no moving parts.

In this work the application of ejector technology to solid oxide fuel cell anodic recirculation, as shown in Fig. 2, is analysed. There are many differences between this application of the ejector and the traditional ones, specifically due to the chemical composition and temperature of the gases and the constraints to be considered. In the present application the primary fluid is fuel (methane or natural gas) preheated to 400–500 °C, while the secondary one is the cell exhaust anodic flow, mainly composed of carbon dioxide and steam at a temperature around 1000 °C [6].

The main goals of the ejector in the SOFC anodic recirculation system are to:

- Maintain fuel cell pressure at the required level, taking into account the pressure losses inside the fuel cell anodic zone and reformer.
- Recirculate sufficient secondary mass flow to obtain the proper operation of the reformer.
- Recirculate sufficient secondary flow to have an apt steam to carbon ratio to avoid carbon deposition in the cell and in the reformer. In fact to avoid carbon deposition the ratio between the primary flow (fuel) and the secondary one may be very high, usually higher than in ejector systems for traditional applications.

2. SOFC anodic recirculation with ejectors

As already stated, the main objective of the ejector recirculation system is to recirculate part of the anodic exhaust

* Corresponding author. Tel.: +39-010-3532444; fax: +39-010-3532566.
E-mail address: massardo@unige.it (A.F. Massardo).
[1] http://www.tpg.unige.it.

0378-7753/$ – see front matter © 2003 Elsevier B.V. All rights reserved.
doi:10.1016/j.jpowsour.2003.11.034

Nomenclature

c	velocity
c_p	specific heat at constant pressure
c_v	specific heat at constant volume
Cp	$\frac{p_4-p_3}{\rho_3 c_3/2}=\left(1-\left(\frac{\Omega_4}{\Omega_3}\right)^{-2}\right)-\frac{\text{losses}}{\rho_3 c_3/2}$
CP	constant pressure
Cpi	$\frac{p_{t_3}-p_3}{\rho_3 c_3/2}=\left(1-\left(\frac{\Omega_4}{\Omega_3}\right)^{-2}\right)$
CS	constant section
E_c	kinetic energy
F	$\dot{m}_2/\dot{m}_1$
h	enthalpy
i	current
$m, \dot{m}$	mass flow rate
M	Mach number
N	mole number
p	pressure
R	gas constant
S	entropy
T	temperature
U_f	$\frac{\text{utilized fuel}}{\text{total inlet fuel}}=\frac{H_{2_{in}}-H_{2_{out}}}{H_{2_{in}}}$

Greek letters

β	pressure ratio
γ	c_p/c_v
η	efficiency
ρ	density
Ω	area

Subscripts

cr	critical conditions
diff	diffuser
m	average value
t	total
th	nozzle throat
1	mixing section inlet—primary fluid
1_{in}	primary fluid inlet
2	mixing section inlet—secondary fluid
2_{in}	secondary fluid inlet
3	diffuser inlet
4	diffuser outlet

flow through the injection of fuel (primary flow), mainly to:

- Obtain sufficient sensible heat necessary for the reforming reaction [7].
- Maintain the cell pressure as required by the hybrid system operation.
- Meet the so-called steam to carbon ratio, defined as follows:

$$\text{STCR}=\frac{n(\text{H}_2\text{O})}{n(\text{CO})+n(\text{CH}_4)} \tag{1}$$

In fact, in a fuel cell system, it is very important to have enough water vapour to allow the reforming process to take place:

$$\text{CH}_4+\text{H}_2\text{O}\leftrightarrow \text{CO}+3\text{H}_2 \tag{2}$$

$$\text{CO}+\text{H}_2\text{O}\leftrightarrow \text{CO}_2+\text{H}_2 \tag{3}$$

and to avoid the phenomena of CH_4 and CO cracking:

$$\text{CH}_4\leftrightarrow \text{C}+2\text{H}_2 \tag{4}$$

$$2\text{CO}\leftrightarrow 2\text{C}+\text{O}_2 \tag{5}$$

and the consequent carbon atom deposition that poisons the anodic substrate of the fuel cell [7]. Since the anodic exhausts are rich in steam (about 40–45% in mass) and poor in carbon monoxide the recirculation of part of these gases produces enough water vapour in the anodic inlet flow to prevent carbon deposition. On the other hand, the high temperature of the anodic exhausts (in the range of 950–1000 °C) can provide the heat necessary for the endothermic reforming reactions without employing expensive catalysts.

Another solution for anodic recirculation is the use of traditional blowers, as has already been done for molten carbonate fuel cell (MCFC) applications [8,9]. This case is less risky, taking into account that the recirculation is carried out at a temperature just over 650 °C while, as already stated, the temperature is quite close to 1000 °C for SOFCs. On the other hand, the ejector operates without moving parts, so it has to face considerably lower stress, can be realised using more conventional materials, and it does not need lubrication, avoiding problems of anode poisoning [10].

Taking these points into account, the use of ejectors for SOFC anode recirculation increases the reliability of the whole hybrid system when compared to the blower solution.

3. Design of the ejector

To determine the ejector design, the design-point operative conditions of the fuel cell must be known (cell operative pressure, pressure losses, exhaust chemical composition and temperature). As an example Table 1 shows the typical values obtained for a SOFC hybrid system analysed by the authors [11]. Starting with these data the main task of the design-point calculation is the evaluation of the ejector geometry and the primary flow (fuel) pressure necessary to satisfy the hybrid system specifications (mass flow ratio, steam to carbon ratio, reformer operating temperature).

The ejector design model is based on energy, continuity and momentum equations:

$$\text{energy}:\quad \dot{m}_1\left(h_1+\tfrac{1}{2}c_1^2\right)+\dot{m}_2\left(h_2+\tfrac{1}{2}c_2^2\right)=\dot{m}_3\left(h_3+\tfrac{1}{2}c_3^2\right) \tag{6}$$

$$\text{continuity}:\quad \dot{m}_1+\dot{m}_2=\rho_3 c_3 \Omega_3 \tag{7}$$

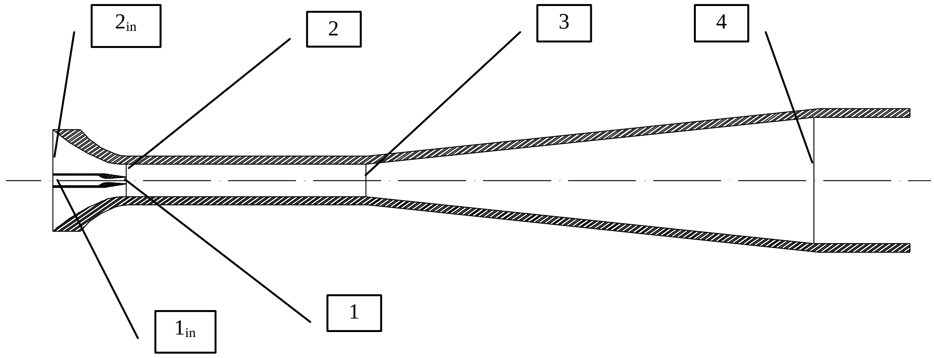

Fig. 1. Supersonic nozzle ejector scheme.

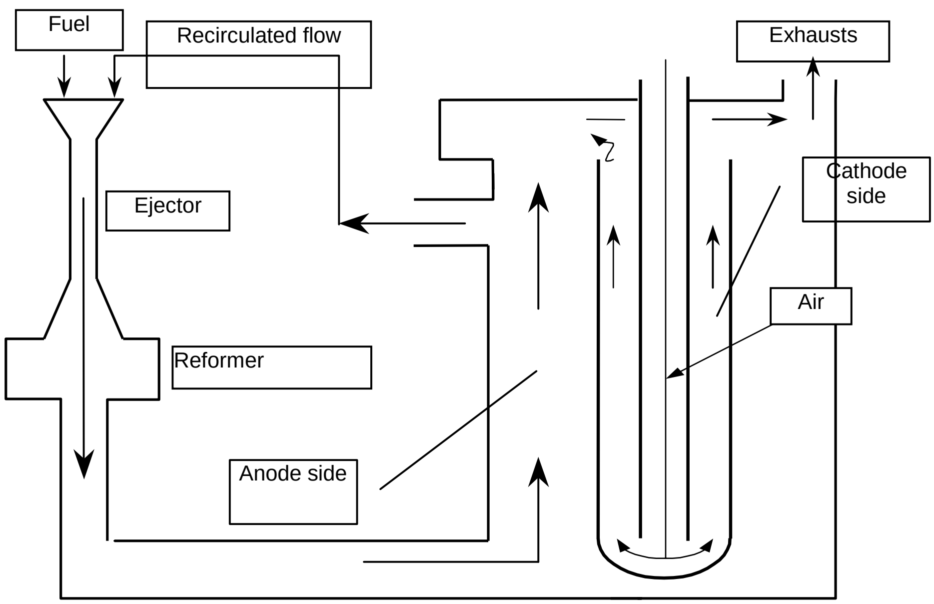

Fig. 2. Anodic circuit of a tubular SOFC.

$$\text{momentum}: \quad p_3\Omega_3 - p_1\Omega_1 - p_2\Omega_2 - \int_{1-2}^{3} p\,\mathrm{d}\Omega = \dot{m}_1c_1 + \dot{m}_2c_2 - \dot{m}_3c_3 \qquad (8)$$

To define the geometry of the ejector the fluid dynamic phenomena are considered adiabatic, taking into account the irreversibilities with apt coefficients for expansion, mixing and compression zones [10]. The solution is based on an iterative method: the outlet static pressure (p_4) is evaluated for a defined geometry and compared with the required value. The difference between these two values is used to adjust primary flow pressure and ejector geometry until convergence is reached.

Two different geometries have been investigated, the first one represents a constant mixing section ejector, the second one a constant mixing pressure ejector, in order to compare them and analyse their main advantages [12]. In this phase, taking into account the data of Table 1, some parameters were fixed according to fuel cell and hybrid system requirements: in particular a pressure loss equal to 1.5% of the cell operating pressure. A design value of steam to carbon ratio equal to 2.4 and a lower limit equal to 1.8 were considered reasonable to avoid carbon deposition [9]. The fuel inlet temperature was assumed to be equal to 400 °C (673 K),

Table 1
Design-point values

FC power (kW)	250
FC anodic temperature (K)	1280
Fuel inlet temperature (K)	673
Chemical composition (mass, %) of anodic exhausts	
H_2	0.39
CO_2	51.46
CO	4.19
H_2O	43.96
Fuel composition (mass, %)	
CH_4	100
Fuel flow rate (kg/s)	0.0094
FC pressure (kPa)	380
FC pressure losses (kPa)	5.7

depending on the fuel preheater operation. The secondary flow inlet diameter (Section 2) was imposed to obtain a proper Mach number at design conditions [14] (compromise between the need for high velocity to enhance the mixing process, and that of reducing average flow velocity to limit the losses in the diffuser). The mixing duct length was assumed to be 10 times the diameter in order to guarantee sufficient space and time for complete mixing, particularly from the point of view of the velocity profile [13]. In fact, it is very important to have a profile as uniform as possible at the diffuser inlet to avoid great differences in the dynamic pressure between the boundaries and axis zone, a circumstance which could lead to the separation of the boundary layer with backflows into the diffuser, a highly dissipative phenomenon. The outlet section of the diffuser is obtained fixing the exit flow velocity at quite a low value, taking into account the proper connection between the reformer and the fuel cell itself. The efficiency of the diffuser (defined as the ratio between the actual static pressure increment and the theoretical one) mainly depends on such factors as the diffuser shape, the ratio between inlet and outlet areas and the flow speed [12]. A conical shape was chosen, even if a trumpet profile would have been preferable from the performance point of view (the risk of boundary layer separation is considerably reduced) but this would have led to complications in the construction of the components, also taking into account the small size of the ejector for SOFC hybrid applications.

These assumptions allow the calculation of the ratio between the secondary and primary flows (fraction, F), and the obtained value is higher than for traditional ejector applications [1–3,13]. It corresponds to a very high fuel inlet pressure value to entrain the required secondary fluid flow rate, and impose the choice of a choked converging–diverging nozzle to reach supersonic speed. Obviously, the ejector outlet temperature and enthalpy, which depend on the ratio between the primary and secondary flows, have been checked to guarantee adequate conversion efficiency in the reformer (see Fig. 2).

The main results obtained for the ejector design-point operation are reported in Table 2. These results are fairly similar for the two configurations; this is a consequence of the low compression ratio and of the relatively low flow speed. The constant area mixing solution produces a light fluid compression because of the oblique compression shock waves generated by the interaction between the supersonic primary flow and the subsonic secondary one. On the other hand, in the constant pressure solution this phenomenon leads to a methane density increase, so the mixing duct is characterised by a first, slightly convergent portion (Fig. 3).

Table 2
Geometry of the ejectors: (i) constant section; (ii) constant pressure

	Constant section	Constant pressure	$\Delta = (\mathrm{CS} - \mathrm{Cp})/\mathrm{CS}$
Nozzle, d_{th} (mm)	3.41	3.31	0.029
Nozzle, d_1 (mm)	3.54	3.47	0.020
d_2 (mm)	21.9	21.9	0
d_3 (mm)	21.9	20.4	0.068
d_4 (mm)	100.8	100.8	0
L_{mix} (mm)	219	219	0
L_{diff} (mm)	450.9	459.5	−0.019
Angle (°)	10	10	0
$p_{1_{in}}$ (kPa)	946	1006	−0.063

4. Ejector off-design performance

Since the thermochemical and pressure conditions in the cell cannot generally be considered fixed, the hybrid system load adjustment is usually carried out by adjusting the fuel flow rate (primary flow rate and, consequently, primary flow pressure) there is an evident need to predict the ejector performance at fuel cell part-load conditions too, to be able to always guarantee the correct behaviour of the anodic side of the fuel cell (particularly the fuel flow rate, STCR, pressure and temperature).

In this way a new code was developed to analyse the ejector off-design performance (fixed ejector geometry, primary flow (fuel) pressure considered a variable input parameter). The results are the pressure, velocity, chemical composition and temperature distribution inside the ejector and the conditions at the ejector outlet (agreeing with reformer inlet conditions). At the beginning the off-design analysis was carried out considering the stand-alone ejector (i.e. separated from the fuel cell), and in this case the secondary flow conditions were assumed to be based on SOFC anodic exhaust behaviour.

As an example, Fig. 4 shows the non-dimensional relationship between the recirculated fraction F and the pressure increase in the ejectors, keeping the primary and secondary flow pressures constant. As in a centrifugal compressor, the pressure ratio decreases as the mass flow increases; the constant section ejector shows a more constant trend. Obviously

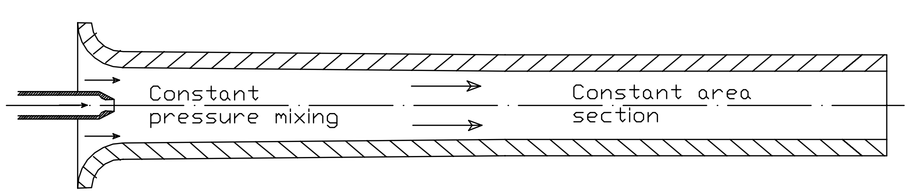

Fig. 3. Constant pressure mixing duct.

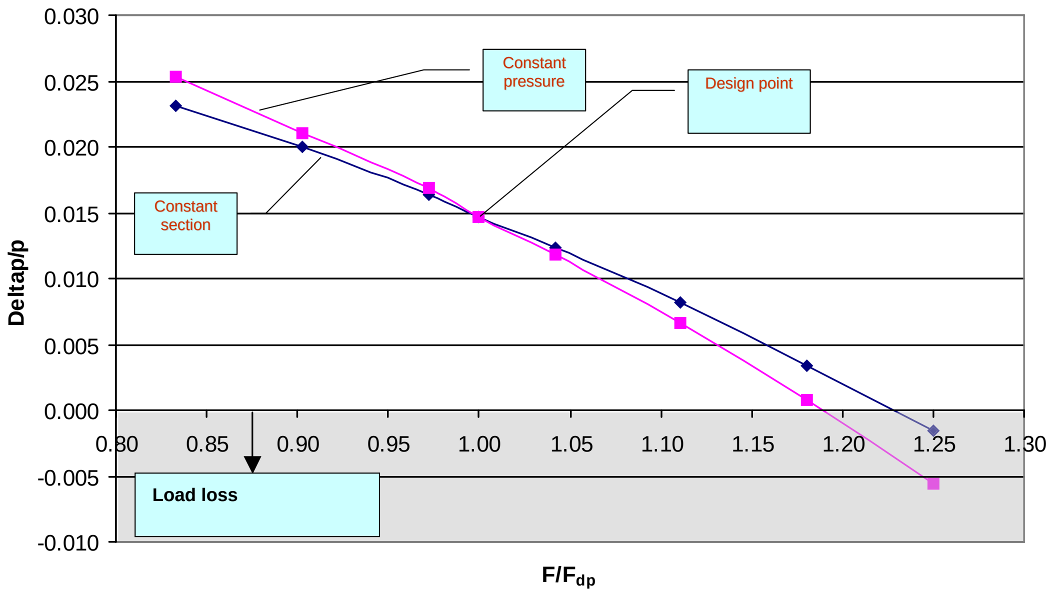

Fig. 4. Non-dimensional characteristic curves for the ejectors ($m_1 = 0.0094$ kg/s, $p_{cell} = 380$ kPa).

Δp is always very small because the main task of the ejector is to maintain the pressure level throughout the flow recirculation in the cell. The figure shows that for an F slightly greater than the design-point value (F_{dp}), the ejector gives a pressure approximately equal to the secondary flow inlet pressure ($\Delta p = 0$): this can be considered as a limit for the correct operation of the ejector and recirculation system.

Other calculations were carried out by modifying the primary flow pressure (and therefore fuel flow rate). In the first calculation, whose results for the constant section ejector are presented in Fig. 5, the F ratio was assumed to be constant and the pressure value was analysed in different ejector sections. The exit pressure (p_4) presents a maximum for a flow rate next to the design-point, while the diffuser inlet total pressure p_{t_3} increases in accord with the fuel pressure. The dotted line represents the flow velocity that increases because the total mass flow rate also rises as $c_3 = \dot{m}/\rho_3 \Omega_3$, where Ω_3 is fixed and ρ_3 is almost constant. In Section 3, when the mass flow rate increases the static pressure decreases because the flow velocity increases as is evident in:

$$p_3 = p_{t_3}\left(1 + M_3{}^2\left(\tfrac{1}{2}(\gamma_3 - 1)\right)\right)^{\gamma_3/(1-\gamma_3)} \quad (9)$$

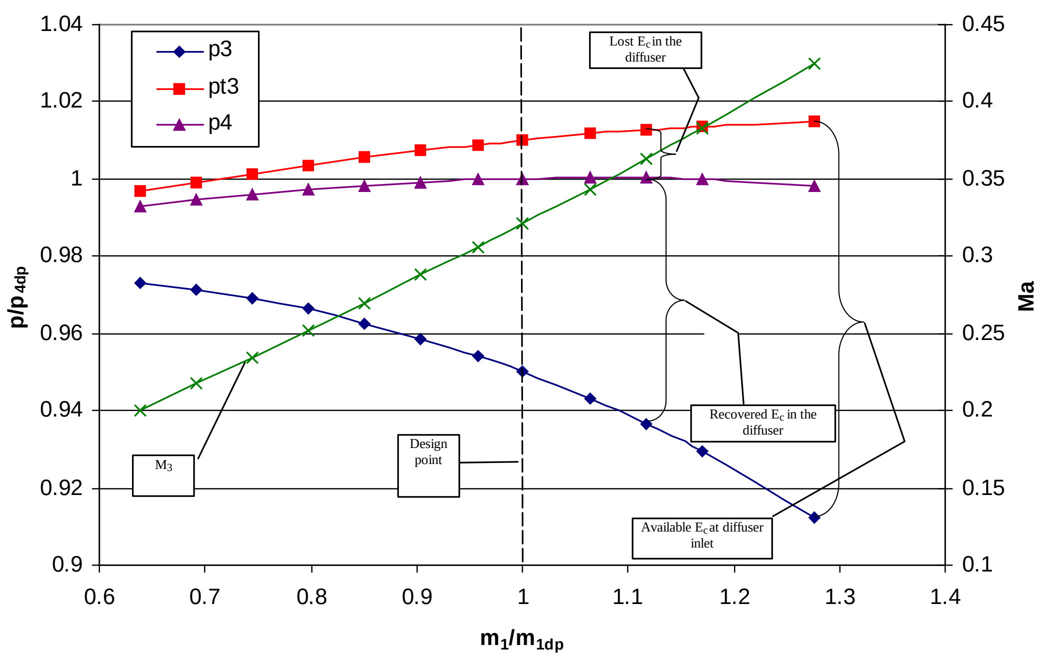

Fig. 5. Total and static pressures and flow speed in different ejector sections ($m_2/m_1 = 7.2$, $p_{cell} = 380$ kPa).

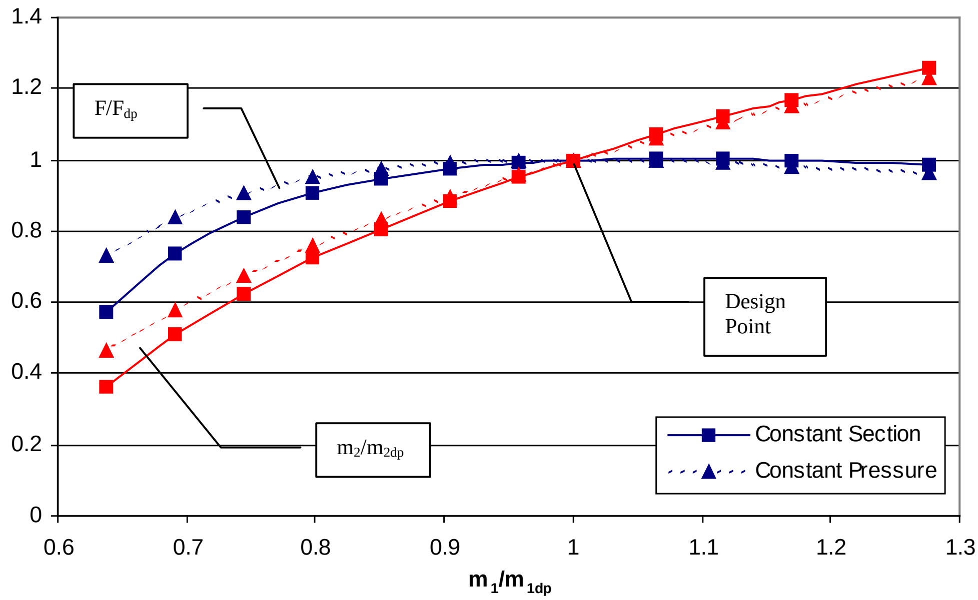

Fig. 6. Recirculated fraction and secondary mass flow rate: comparison of constant section and constant pressure ejectors.

The kinetic term $\rho_3(c_3^2/2)$, that is all the available energy that could be converted to static pressure, can be visualised as the difference between the total and static pressures in the section, while the difference between the static pressures in Sections 3 and 4 represents the actual converted kinetic energy fraction, and the remaining portion is dissipated because of irreversibilities in the diffuser.

In the following case, the secondary flow pressure and ejector exit static pressure were imposed while the recirculated fraction was calculated by varying the primary flow pressure (i.e. fuel flow rate). The calculation was carried out for different inlet pressure values, obtaining a surface for ejector steady operating points. The behaviour of two meaningful parameters such as the F fraction and secondary flow rate is shown in Fig. 6. This increases with the fuel flow rate but the slope of the curve decreases slightly, because of the recirculated fraction trend, similarly to the p_4 obtained for the F constant, due to the relationship between the two parameters (Fig. 4). The difference between the two models is due to the flow speed variation, which is greater in the constant pressure component, involving a steeper curve slope.

Fig. 7 shows the surface made up of ejector steady operating points at different pressures. If the secondary inlet pressure changes, the operating point moves to another curve and reaches another operating condition; unusual for high flow rates, the F ratio decreases by reducing $p_{2_{in}}$: this is due

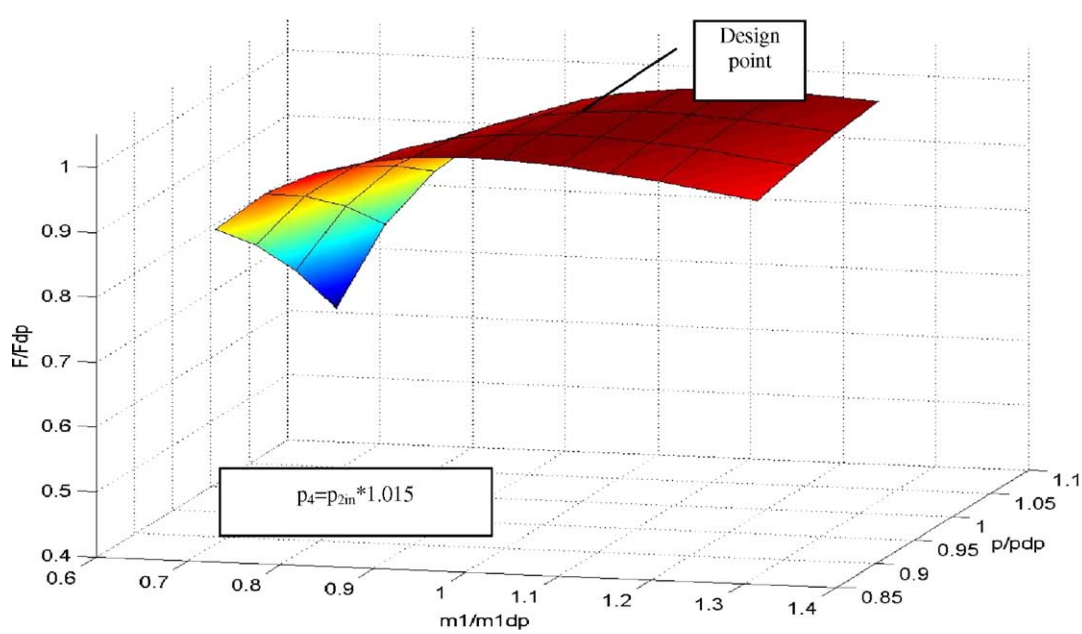

Fig. 7. Recirculated fraction varying fuel flow rate at different operating pressures.

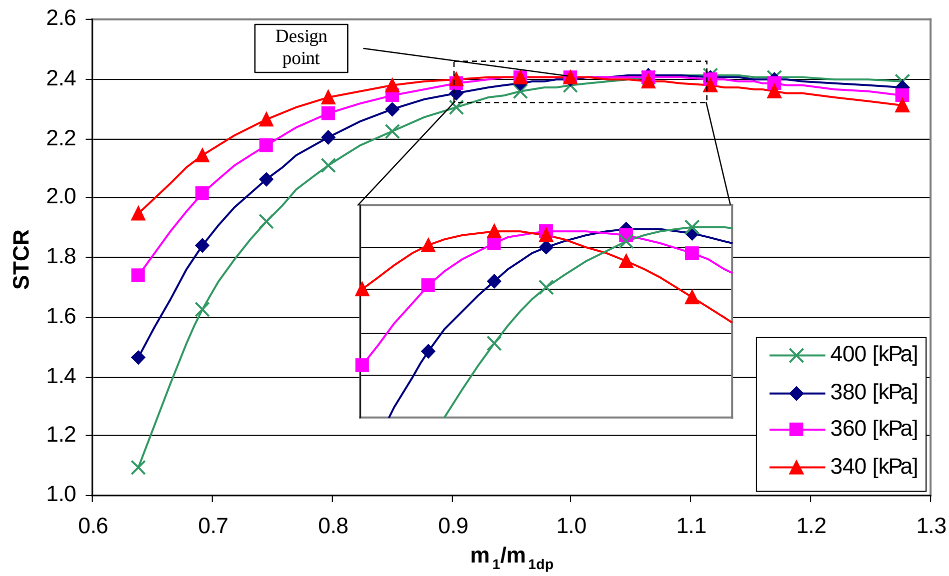

Fig. 8. STCR vs. fuel flow rate at different cell operating pressures.

to the increase in flow speed (in fact, if p, and therefore ρ, diminish, $c = \dot{m}/\rho\Omega$ increases) which leads to higher dissipation. This trend is the opposite of that for a lower flow rate where the influence of the velocity is less important and ejector behaviour is mainly influenced by primary flow energy reduction, which leads to a drop in ejector performance.

It is possible to note how F always shows quite high values: this leads to a reformer inlet temperature that is always sufficiently high (over 1120 K) and the STCR parameter also remains above the limits except that for $m_1/m_{1_{dp}}$, which is lower than 0.7 at high pressure (Fig. 8). In particular, the trend of this parameter is quite similar to the F one. In fact, as the secondary fluid chemical composition is also fixed in this case, the STCR value only depends directly on the F parameter.

Other calculations were carried out varying primary and secondary flow temperatures: obviously the outlet temperature follows the T_1 and T_2 variations (Fig. 9) and, in particular, the fuel temperature has a strong influence on its own flow rate and on entrainment capability. In fact, keeping primary flow pressure constant, the density variation leads to a strong variation in the fuel flow rate and consequently in the total available momentum (Fig. 10).

5. Integration of the ejector recirculation system in the SOFC hybrid model

The final goal of this work is the integration of the ejector recirculation model and the solid oxide fuel cell model

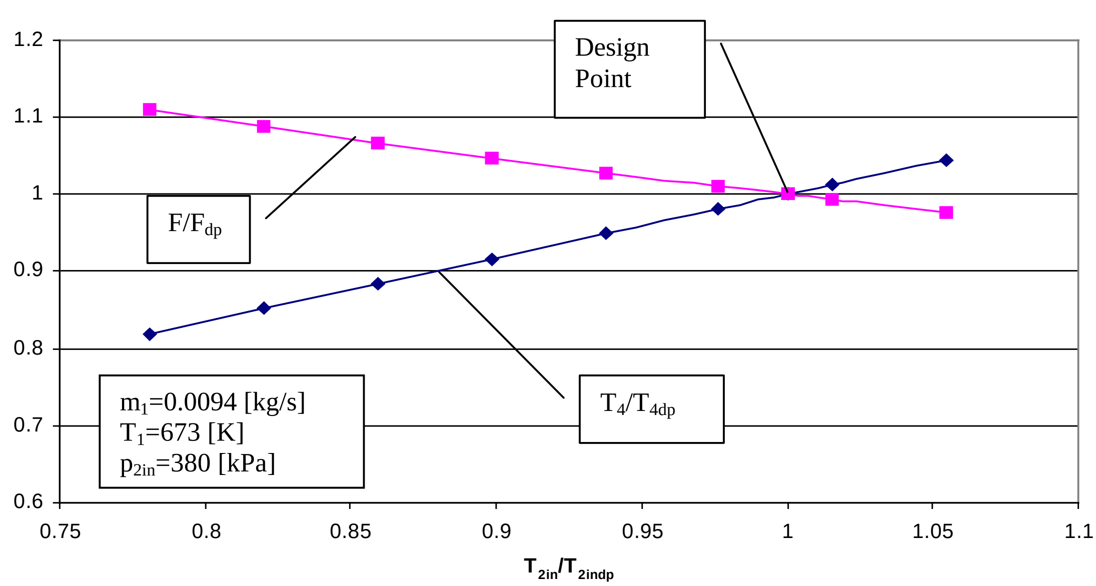

Fig. 9. Outlet temperature and F ratio varying secondary flow temperature.

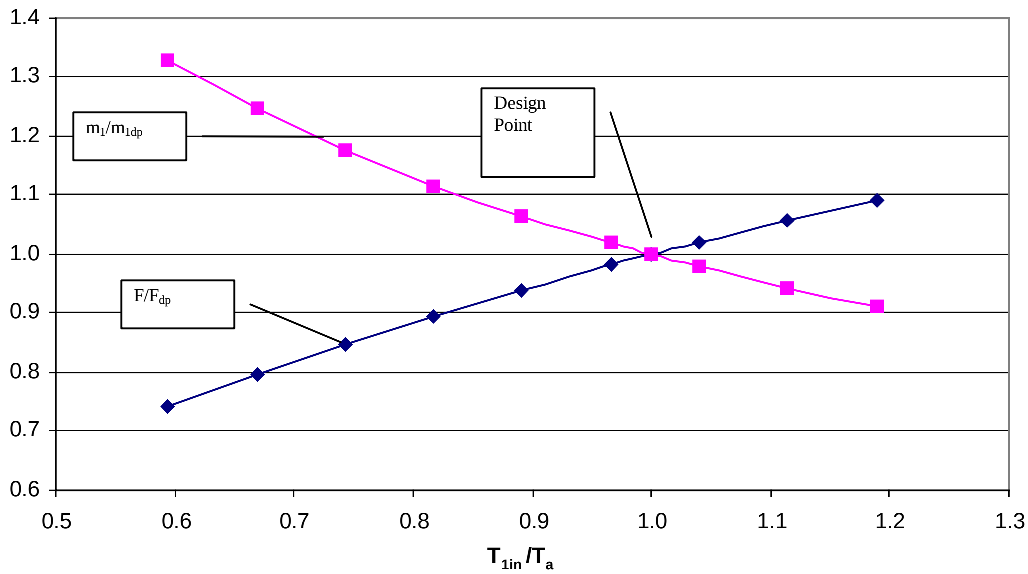

Fig. 10. Fuel flow rate and F ratio varying primary flow temperature.

developed previously by the authors [11], to improve hybrid system performance analysis. In fact, for simplicity in the cited model, the recirculated fraction F was considered constant and always equal to the design-point condition. This simplified assumption led to having the STCR and reformer inlet thermochemical features dependent only on the secondary fluid chemical composition and temperature [12].

In the new integrated model many parameters, such as mixture temperature, chemical composition, pressure and steam to carbon ratio, are calculated by ejector block and used in the fuel cell calculation as shown in Fig. 11. The external loop returns the values of the temperature and chemical composition of the anodic exhausts (ejector secondary flow), which are obviously not constant under the different operating conditions examined, to the ejector. Therefore the calculation is fully iterative.

Calculations for the SOFC anode recirculation system were carried out at different operating points, varying some significant parameters in order to simulate the different hybrid system operating conditions. The ejector outlet pressure was always assumed to be 1.5% greater than the secondary flow one, while the recirculated fraction was calculated each time.

First of all the fuel flow control situation was considered, keeping the cathode air pressure and temperature, fuel composition and temperature, and utilisation factor U_f (imposing current density value) constant while the air flow rate was proportional to the fuel one. The steam to carbon ratio, calculated at different fuel cell pressures, while varying the fuel flow rate, showed a quite similar behaviour (Figs. 12 and 13) to that obtained for the stand-alone ejector. This is due to the fact that working with imposed cell current density, the anode exhaust chemical composition and temperature are subjected to very small variations, which do not seriously affect the STCR; therefore this parameter also mainly depends on the secondary flow rate. It is interesting to note how, on the right side of these figures, when the cell pressure is decreased, the F ratio and STCR decrease too. This behaviour is due to the fluid density increase that considerably affects flow velocity, and so diffuser losses.

The results shown demonstrate that the constant pressure mixing ejector, being more influenced by flow speed variation, presents a higher maximum move leftwards, and a steeper curve slope.

Another very interesting aspect of the analysis is that the ejector behaviour strongly influences the reformer performance too. To analyse this effect the variation in the efficiency of the reforming process, defined as:

$$\eta_{ref} = \frac{n_{CH_4\,in} - n_{CH_4\,out}}{n_{CH_4\,in}} \tag{10}$$

has been considered. This efficiency essentially depends on the temperature and molecular composition of the incoming reformer fluid; in particular the η_{ref} increases with temperature and with H_2O percentage. Recirculated flow is rich in H_2O, so reformer efficiency follows the secondary flow rate trend but presents maximum values moved slightly rightwards (Fig. 14), as the temperature increases at higher primary flow rate. Moreover, it is evident that the η_{ref} is favoured by lower fuel cell pressures, because in this reaction the number of moles increases and high pressures hinder the phenomenon [6].

The results obtained by varying the fuel utilisation factor—U_f varies from 0.65 to 0.88 (0.85 is the design-point value)—at constant fuel cell pressure are reported in Fig. 15. The average temperature (and therefore the anodic exhaust temperature) rises with the U_f and the ΔT in the reformer also increases. This effect is related to the variation in the H_2O percentage at the reformer inlet (dotted line in Fig. 15), due to the different progresses of the electrochemical

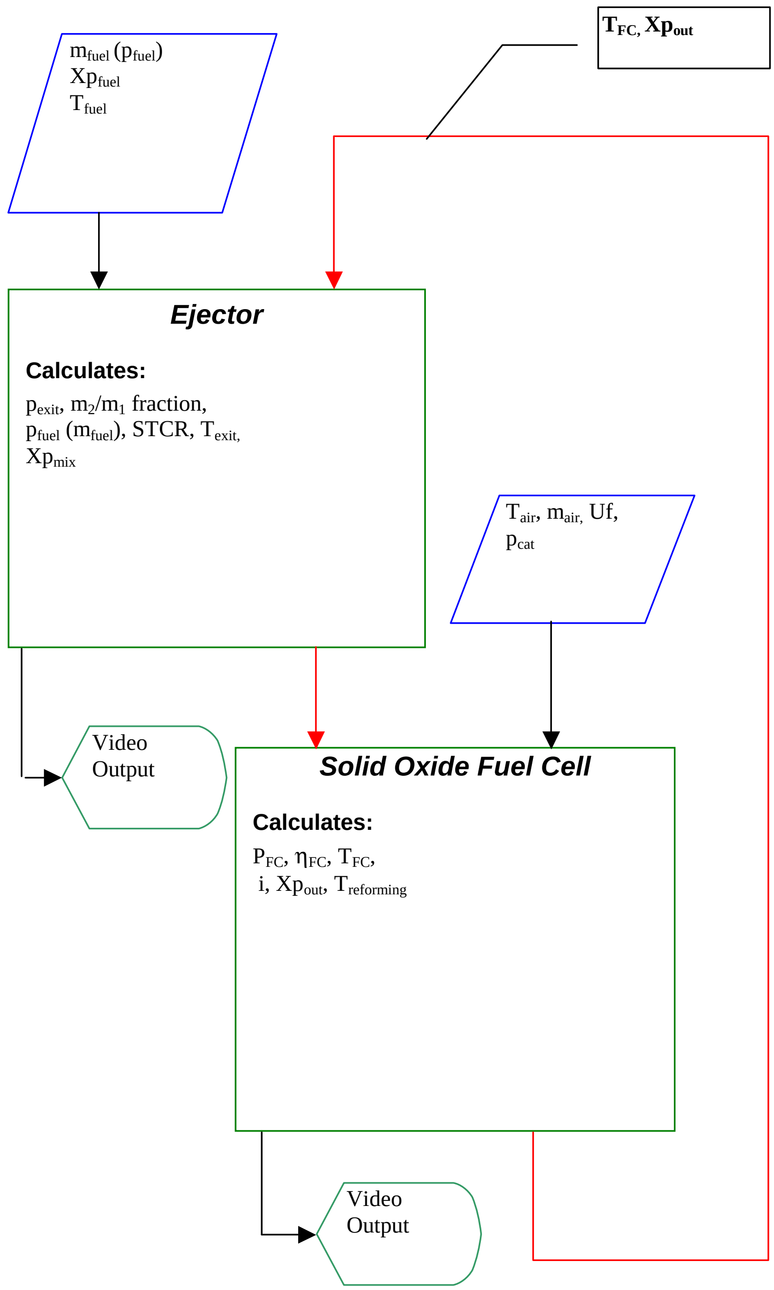

Fig. 11. Simplified data flow scheme of the integrated SOFC-ejector model.

reactions in the cell, and leads to the supposition that there is a different velocity for the reforming process too. In fact, Fig. 16 shows a large difference, as $U_f = 0.88$ and 0.65. Also in this case the entrainment capability of the ejector is strongly influenced by the chemical composition and temperature variation, as shown by the other line in Fig. 16. The simultaneous reduction of entrainment capability and H_2O percentage at low utilisation factors, together with the increase in the CO concentration due to the reduced progress of the electrochemical reactions, lead to problems related to the STCR parameter. In fact, Fig. 17 confirms that, for a U_f lower than 0.7, the STCR can easily drop below the limit value, with an evident risk of carbon deposition.

The new anode recirculation system model has been compared with the previous one [11], where the ejector was modelled in a simplified way. The input data utilised in the simulation are summarised in Table 3. In this comparison only constant section ejector results have been considered for reasons of simplicity. In this way the influence of the ejector design and off-design performance on the whole hybrid system may be obtained and discussed.

The most important comparison obviously concerns the anodic flow rate is shown in Fig. 18. Using the simplified

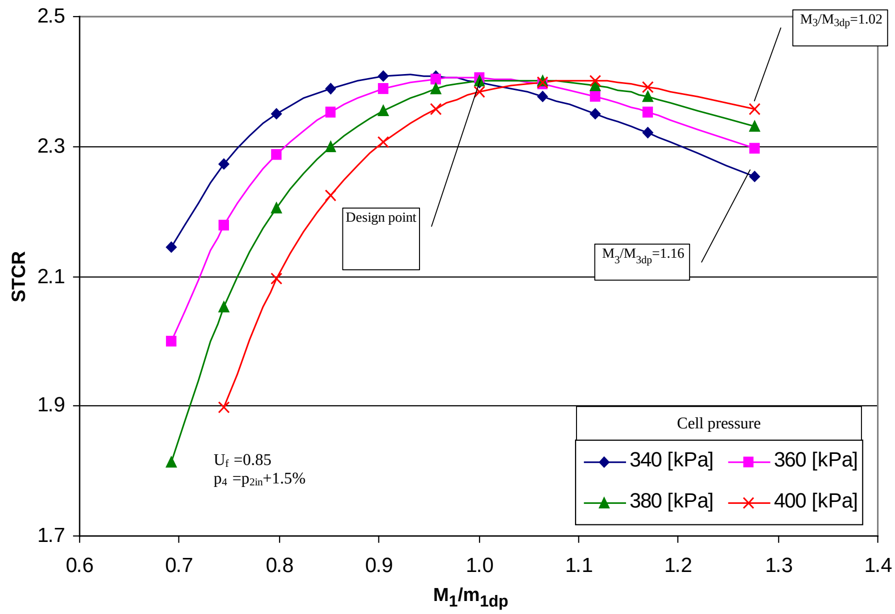

Fig. 12. STCR parameter—constant section mixing duct ejector.

Table 3
Comparison of old and new models

SOFC with present ejector model		SOFC with simplified ejector model	
Fuel	CH_4	Fuel	CH_4
T_{fuel} (K)	673	T_{fuel} (K)	673
T_{air} (K)	878	T_{air} (K)	878
p_{cell} (kPa)	380	p_{cell} (kPa)	380
$\Delta p_{ejector}$ (kPa)	5.7	$\Delta p_{ejector}$	Not calculated
m_2/m_1	Variable	m_2/m_1	7.2 (fixed)
U_f	0.85	U_f	0.85

model, where the ejector was considered to always be able to provide the F ratio value defined for the design-point, the total anodic flow rate varies linearly with the fuel flow rate (see dotted line in Fig. 18). On the contrary, using the complete new model the anodic total flow is subjected to a variation, since the recirculated fraction depends on the ejector performance. The STCR is also quite different, strictly depending on the recirculated fraction, but in the analysed conditions it always remains within the safety limits. It is interesting to note how, in the previous model, the STCR was not exactly constant, even if F was fixed, since the exhaust chemical composition was not fixed during the fuel cell regulation.

The differences in the operation of the reformer are quite evident: in fact with the simplified approach its operation depends only on the inlet flow (ejector exhaust) temperature (chemical composition was almost constant). With the new complete approach the curve depends on both the temperature and recirculated fraction composition values (Fig. 19), whose trend affects the operation of this component, as already discussed.

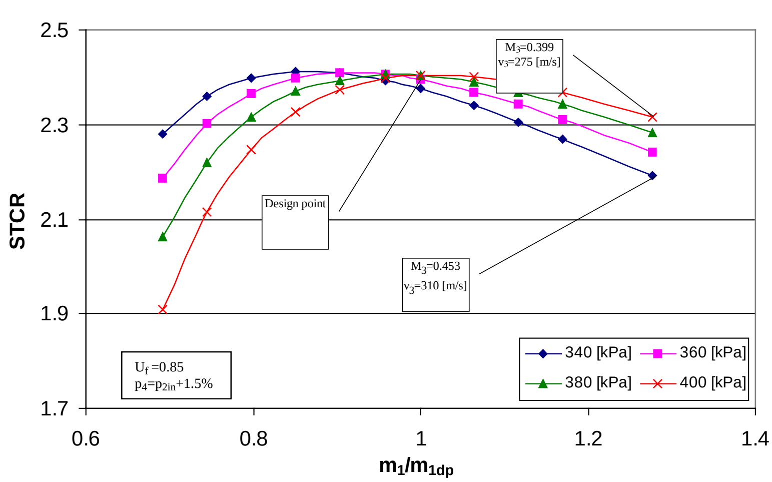

Fig. 13. STCR parameter—constant pressure mixing duct ejector.

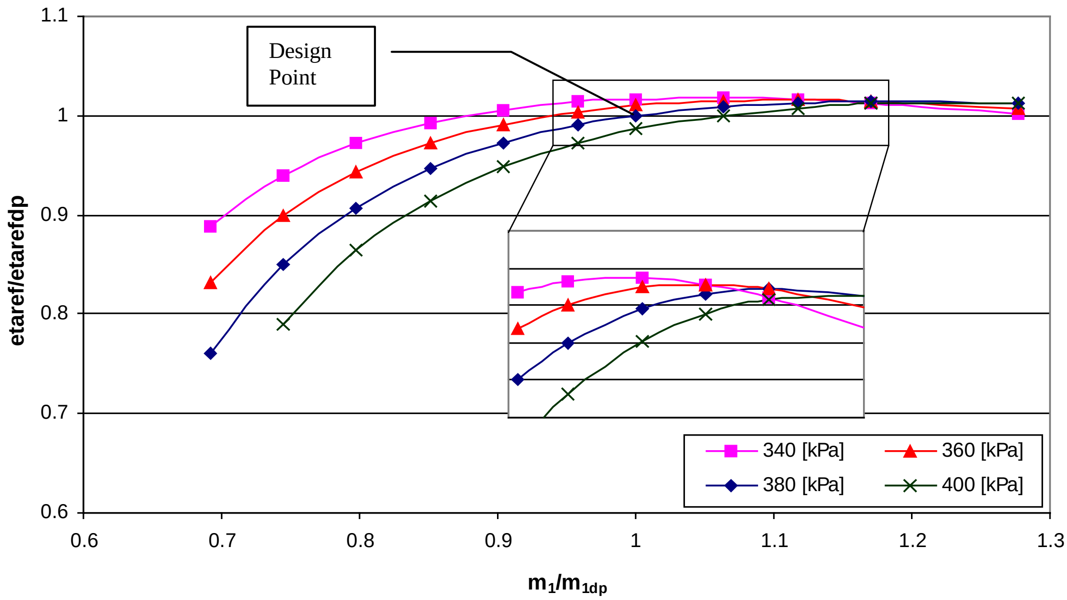

Fig. 14. Reformer efficiency (constant section ejector).

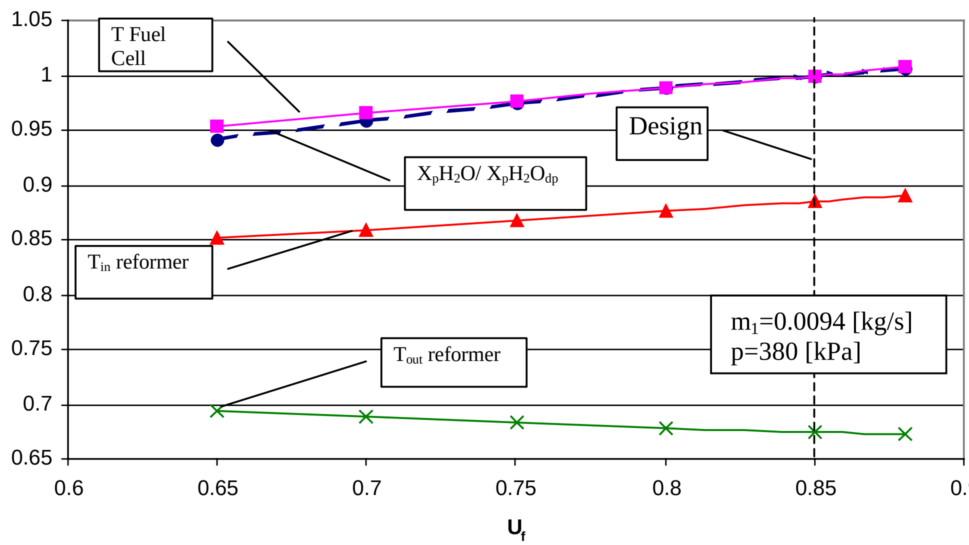

Fig. 15. Temperatures (adimensionalised on $T_{FC_{dp}}$) and H_2O percentage in anodic exhausts.

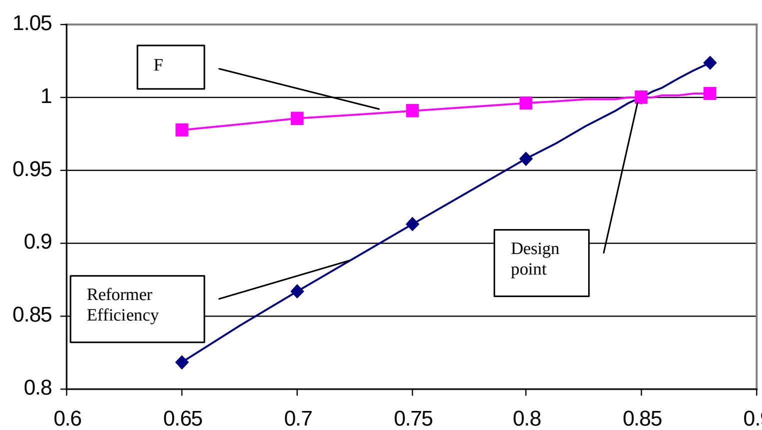

Fig. 16. Reformer efficiency and entrained fraction vs. U_f (constant section ejector).

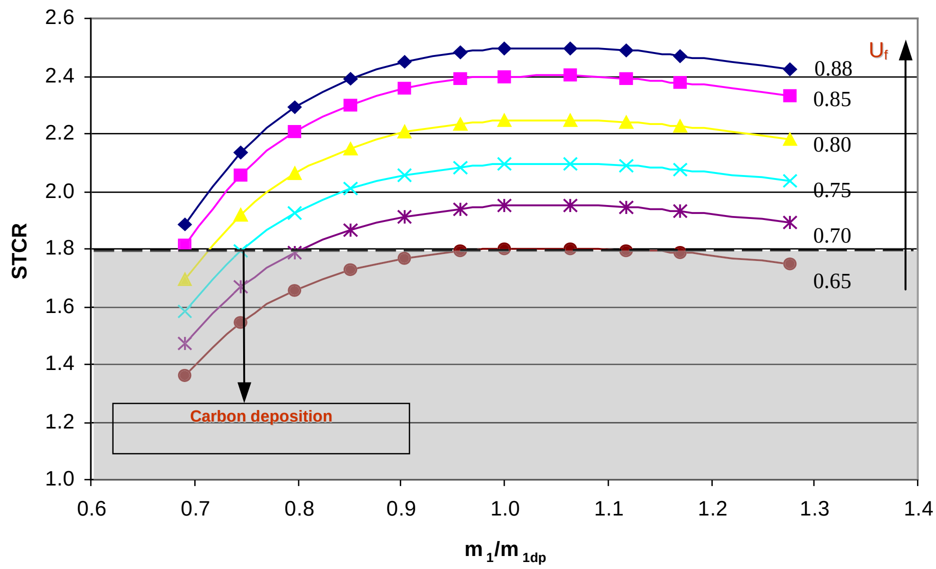

Fig. 17. STCR trend at different utilisation factors varying fuel flow rate (constant section ejector).

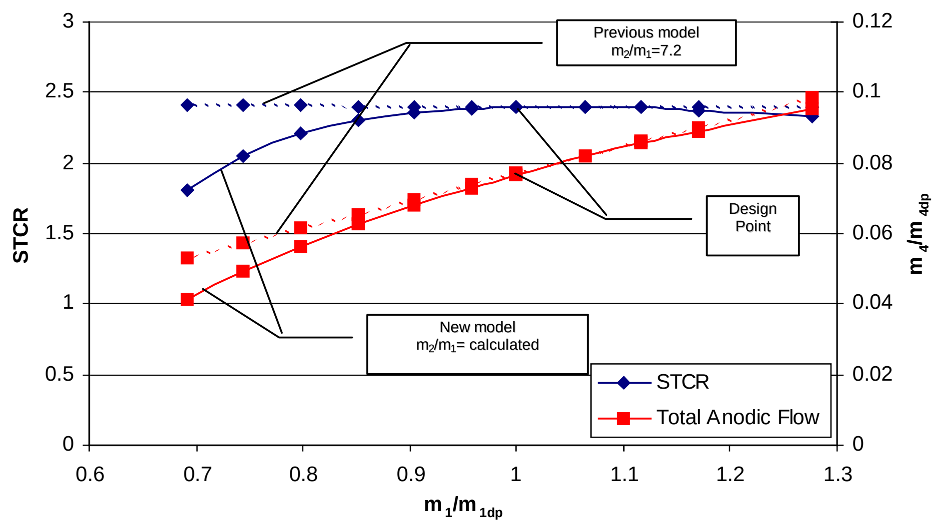

Fig. 18. Comparison of old and new models.

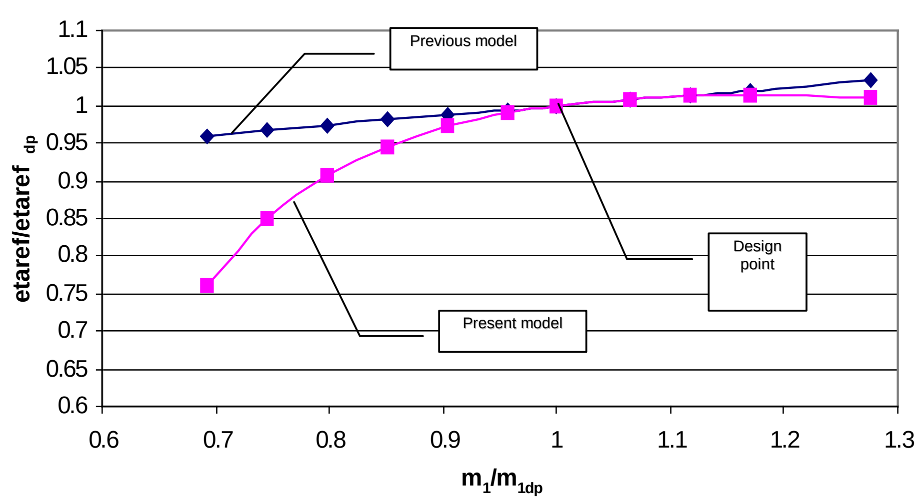

Fig. 19. Reformer efficiency.

6. Conclusions

The design and off-design performance of an ejector anodic recirculation system for SOFC hybrid applications has been presented and analysed.

Two different ejector geometries have been investigated: (i) constant pressure mixing section; (ii) constant area mixing section. A complete design-point analysis has been presented for both on the basis of data coming from a previously investigated SOFC hybrid system.

The ejector has been designed to satisfy the following requirements: (a) supply the sensible heat necessary to reformer reaction through anodic flow recirculation; (b) maintain the cell pressure at the required value for proper hybrid system operation; (c) verify the steam to carbon ratio through the proper recirculation of water present in the anodic exhaust.

In the second part of the paper the off-design performance of the ejector in two different configurations—stand-alone or integrated with the SOFC system—has been carefully investigated, taking into account that one of the main control parameters for the part-load operation of the hybrid system is the fuel flow rate, i.e. the ejector primary flow pressure.

The results obtained allow the following main conclusions to be stated:

1. The performance of the anodic recirculation system is quite similar when using different ejector geometries due to the very low pressure increase and the large flow ratio F required from the ejector (Figs. 4 and 6).
2. The steam to carbon ratio constraint is the most stringent one, and it is verified in most cases investigated here. Problems may occur at a low fuel inlet pressure or at low U_f values (Figs. 8, 12, 13 and 18).
3. Secondary and primary flow temperature influence has been clarified (Figs. 9 and 10).
4. The influence of the ejector performance on the reformer behaviour has been demonstrated (see Figs. 14 and 16).
5. The off-design performance of the anodic recirculation system integrated with the SOFC for both fixed and variable fuel utilisation factors has shown that for a reduction in U_f the STCR variation is quite large and in the direction of the lower limit (STCR $= 1.8$).
6. The utilisation of a complete ejector simulation in the whole SOFC hybrid has shown that it is now possible to properly take into account all the variations in the STCR and reformer efficiency, due to the iterative calculation between ejector and reformer-cell.

Finally, it is important to note that in the present analysis the conditions on the cathodic side of the cell have been considered fixed. This is a useful simplification to better understand the anodic recirculation behaviour. However, in the actual pressurised SOFC hybrids the off-design variation in the pressure on the cathodic side, due to the pressurisation sub-system (compressor-gas turbine) off-design behaviour, needs an adequate variation in the pressure on the anodic side too. This variation strongly depends on the ejector primary flow pressure and the ejector off-design behaviour. Therefore the off-design and control system of the anodic recirculation system must be carefully designed and verified, also taking into account the constraints on the pressure difference between anode and cathode.

The results presented here represent only a first step towards the complete off-design and transient analysis of the whole SOFC hybrid system.

Acknowledgements

This work has been partially sponsored by MIUR of Italy, through Contract FISR-2000, number 10/02/2003-837, national coordinator A. Massardo.

References

[1] N.H. Johannesen, Ejector theory and experiments, Transactions of the Danish Academy of Technical Sciences, ATS No. 1, 1951.
[2] Y.-M. Chen, Cung, Experimental study of the performance characteristic of a steam-ejector refrigeration system, Exp. Therm. Fluid Sci. 15 (1997) 384–394.
[3] D.W. Sun, I.W. Eames, S. Aphornratana, Evaluation of a novel combined ejector-absorption refrigeration cycle. I. Computer simulation, Int. J. Refrigeration 19 (1996) 172–180.
[4] A. Massardo, M. Marini, A. Satta, M. Geraci, Low area ratio aircraft fuel jet-pump performance with and without cavitation, Trans. ASME 114 (1992) 626–631.
[5] H.G. Elrod, The theory of ejectors, J. Appl. Mech. A 67 (1945) 170–174.
[6] L. Magistri, Hybrid systems for distributed power generation, Ph.D. Thesis, 2003.
[7] T. Takeguchi, et al., Study on steam reforming of CH_4 and C_2 hydrocarbons and carbon deposition on Ni-YSZ cermets, J. Power Sources 112 (2002) 588–595.
[8] O. Grillo, L. Magistri, A.F. Massardo, Hybrid system for distributed power generation based on pressurisation and heat recovering of an existing 100 kW_e molten carbonate fuel cell, J. Power Sources 115 (2003) 252–267.
[9] A.F. Massardo, B. Bosio, Assessment of molten carbonate fuel cell models and integration with gas–steam cycles, ASME Trans., J. Gas Turbines Power 124 (2002) 103–109.
[10] EG&G Services-Parson, Inc. Science Application International Corporation, Fuel Cell Handbook, 5th ed., US DOE, 2000.
[11] P. Costamagna, L. Magistri, A.F. Massardo, Design and part load performance of a hybrid system based on a solid oxide fuel cell reactor and a micro gas turbine, J. Power Sources 96 (2001) 352–368.
[12] F. Marsano, Simulazione del circuito lato anodo di una cella a combustibile ad ossidi solidi per applicazioni in sistemi ibridi, Thesis for Degree of Licentiate in Engineering, 2002.
[13] J.H. Keenan, E.P. Neumann, F. Lustwerk, An investigation of ejector design by analysis and experiment, in: Proceedings of the Annual Meeting on ASME, 1949, pp. 299–309.
[14] A. Ferro, Analisi teorica e sperimentale sul comportamento degli eiettori a fluidi compressibili, Il calore n.3 (1954) 119–128;
A. Ferro, Analisi teorica e sperimentale sul comportamento degli eiettori a fluidi compressibili, Il calore n.4 (1954) 165–181.